Hydrophilic Segmented Block Copolymers Based on Poly(ethylene oxide) and Monodisperse Amide Segments

DEBBY HUSKEN,* JAN FEIJEN, REINOUD J. GAYMANS

Department of Science and Technology, University of Twente, 7500 AE Enschede, The Netherlands

Received 12 April 2007; accepted 26 April 2007
DOI: 10.1002/pola.22186
Published online in Wiley InterScience (www.interscience.wiley.com).

ABSTRACT: Segmented block copolymers based on poly(ethylene oxide) (PEO) flexible segments and monodisperse crystallizable bisester tetra-amide segments were made via a polycondensation reaction. The molecular weight of the PEO segments varied from 600 to 4600 g/mol and a bisester tetra-amide segment (T6T6T) based on dimethyl terephthalate (T) and hexamethylenediamine (6) was used. The resulting copolymers were melt-processable and transparent. The crystallinity of the copolymers was investigated by differential scanning calorimetry (DSC) and Fourier Transform infrared (FTIR). The thermal properties were studied by DSC, temperature modulated synchrotron small angle X-ray scattering (SAXS), and dynamic mechanical analysis (DMA). The elastic properties were evaluated by compression set (CS) test. The crystallinity of the T6T6T segments in the copolymers was high (>84%) and the crystallization fast due to the use of monodisperse tetra-amide segments. DMA experiments showed that the materials had a low T_g, a broad and almost temperature independent rubbery plateau and a sharp flow temperature. With increasing PEO length both the PEO melting temperature and the PEO crystallinity increased. When the PEO segment length was longer than 2000 g/mol the PEO melting temperature was above room temperature and this resulted in a higher modulus and in higher compression set values at room temperature. The properties of PEO-T6T6T copolymers were compared with similar poly(propylene oxide) and poly(tetramethylene oxide) copolymers. © 2007 Wiley Periodicals, Inc. J Polym Sci Part A: Polym Chem 45: 4522–4535, 2007

Keywords: hydrophilic; poly(ethylene oxide); segmented block copolymer

INTRODUCTION

Thermoplastic elastomers (TPE's) are polymers that show elastomeric behavior at their service temperature and can be melt-processed at elevated temperatures. Segmented block copolymers are a kind of TPE's. Generally, segmented block copolymers, composed of alternating rigid and flexible segments, have a two-phase structure. One phase consists of mobile chains with a low glass transition temperature (T_g), the other of crystalline domains with a high melting temperature. The crystalline domains act as physical crosslinks and can be considered as filler, reinforcing the amorphous matrix. Because of the presence of physical crosslinks the materials have good elastic properties.

The T_g of the soft phase depends on the type and length of the flexible segments and on the amount of rigid segment dissolved in the soft phase. Materials of interest have a low T_g and high melting temperature. These materials have a wide rubbery plateau and thus a wide service

Present address: DSM resins, Zwolle, The Netherlands.
Correspondence to: R. J. Gaymans (E-mail: r.j.gaymans@utwente.nl)

Journal of Polymer Science: Part A: Polymer Chemistry, Vol. 45, 4522–4535 (2007)

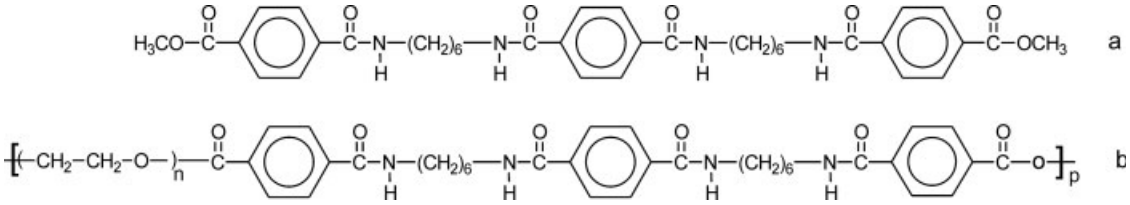

Figure 1. Structure of bisester tetra-amide segment T6T6T-dimethyl (a) and PEO_x-T6T6T (b).

temperature. Often used flexible segments with a low T_g are polyethers, like poly(tetramethylene oxide) (PTMO), poly(propylene oxide) (PPO), or poly(ethylene oxide) PEO. The high melting crystalline domains provide the material dimensional stability, heat stability and solvent resistance. Crystallizable segments that have a high melting temperature contain usually urethanes, esters, or amides groups.

In literature several segmented block copolymers based on flexible PEO segments and ester,[1–3] amide[4,5] or urethane[6–10] types of rigid segments are reported. The PEO-based copolymers are used for breathable film applications, like gloves, laminates on textile, roofing membranes, gas separation membranes or food packaging materials. Furthermore, these copolymers are considered for various biomedical applications, like tissue engineering[11–15] and controlled drug release systems.[16,17]

The crystallinity of the rigid segments in these PEO-based segmented block copolymers is usually low (~30%),[18,19] which means that a large amount of the rigid segments is amorphous and partially dissolved in the PEO matrix. Therefore, these copolymers have at least a three-phase morphology; a crystalline rigid phase and two amorphous phases. The T_g of the PEO phase is low but increases when the content of noncrystallized rigid segments dissolved in the PEO matrix increases. Besides, a second T_g is observed that originates from the amorphous rigid phase. When the concentration and length of the PEO segments increase, the PEO segments tend to crystallize, creating an extra crystalline phase in the copolymer with a low melting temperature.[20]

The crystallization of the rigid segments can be improved by using monodisperse crystallizable segments.[21,22] These monodisperse segments crystallize fast and almost completely. Consequently, there is hardly any noncrystallized rigid segment dissolved in the soft phase. A low amount of monodisperse rigid segments (~5 wt %) is already sufficient for good mechanical and elastic properties of the copolymer.

The use of monodisperse crystallizable segments in segmented block copolymers containing urethane(urea)[23–26] or amide groups[27–33] has been previously studied. These copolymers have a low under-cooling, a relative high modulus and an almost temperature independent rubbery plateau. Besides, these polymers have a high elasticity and high fracture strains. The copolymers can consist of PTMO or PPO flexible segments and bisester tetra-amide rigid segments (T6T6T).[28,30,32] The monodisperse T6T6T segments are based on dimethyl terephthalate (T) and hexamethylenediamine (6)[31,34] [Fig. 1(a)].

The crystallized T6T6T segments have a ribbon-like structure with a high aspect ratio (L/D $\approx$ 1000) dispersed in the polyether matrix.[28,32] The strong increase in modulus with T6T6T content can be described by the composite model of Halpin–Tsai.[32,33] This suggests that the function of the crystalline segments as reinforcing filler is important for obtaining a copolymer with a high modulus. By increasing the T6T6T concentration in the PTMO-T6T6T and PPO-T6T6T copolymers, the storage modulus of the rubbery plateau and the flow temperature (melting temperature) were increased. The storage moduli of the rubbery plateau were similar for both polyether-T6T6T copolymers, but the flow temperatures of PPO-T6T6T were lower than those of PTMO-T6T6T. Furthermore, both copolymers have comparable low compression set (CS) values (6%–17%).

The purity of the T6T6T segments is important as it affects the monodispersity of the rigid segments in the polymer. Previous research on the use of tetra-amide rigid segments in segmented block copolymers shows that with an increased dispersity of the rigid segments, the mechanical and elastic properties of the copolymers deteriorate.[28,29,33]

Both PTMO and PPO polyether segments are hydrophobic and it is interesting to study seg-

mented block copolymers based on hydrophilic PEO segments and monodisperse T6T6T segments [Fig. 1(b)]. This article is directed to the synthesis and characterization of segmented block copolymers based on PEO segments and monodisperse crystallizable T6T6T segments. In forth coming articles the water absorption, the water vapor transport, the gas transport, and the surface properties are presented.

A polymer series, denoted as PEO_x-T6T6T will be prepared where the molecular weight of the PEO segments (x) is varied between 600 and 4600 g/mol. By using Fourier Transform Infrared (FTIR), information is obtained about the PEO and T6T6T crystallization in the copolymer. synchrotron small angle X-ray scattering (SAXS) experiments are used to study the polymer morphology. Phase transitions and thermal mechanical behavior are studied with differential scanning calorimetry (DSC) and dynamic mechanical analysis (DMA), respectively. The elastic behavior is investigated with a compression set test. Interesting is to see what the effect of the highly polar PEO is on the melting temperature of the T6T6T segments.

EXPERIMENTAL

Materials

1,6-Hexamethylenediamine (HMDA) was obtained from Aldrich. Dimethyl terephthalate (DMT) and *N*-methyl-2-pyrrolidone (NMP) were purchased by Merck. Tetra-isopropyl orthotitanate (Ti(i-$OC_3H_7)_4$) was obtained from Aldrich and diluted in *m*-xylene (0.05 M) received from Fluka. Irganox 1330 was obtained from CIBA. Methyl phenyl terephthalate (MPT) was synthesized from phenol (obtained from Aldrich) and methyl-(4-chlorocarbonyl)benzoate (obtained from Dalian).[34] Difunctional poly(ethylene glycol)s (M_n of 600, 1000, 1500, 2000, 3400, and 4600 g/mol) were obtained from Aldrich and were denoted as PEO_x wherein x stands for their molecular weight.

Polymerization of PEO_x-T6T6T Block Copolymers

The PEO_x-T6T6T block copolymers were synthesized by a polycondenzation reaction using PEO segments of different lengths and T6T6T-dimethyl. The T6T6T-dimethyl segments were prepared prior to the polymerization according to the synthesis described by Krijgsman et al.[34] The synthesis of the PEO_{2000}-T6T6T block copolymer is given as an example.

The reaction was carried out in a 250 mL stainless steel vessel equipped with a magnetic stirrer and nitrogen inlet. The vessel contained T6T6T-dimethyl (10 mmol, 6.86 g), PEO_{2000} (10 mmol, 20.0 g), Irganox 1330 (0.20 g), 50 mL NMP, and catalyst solution (1.0 mL of 0.05 M Ti-(i-$(OC_3H_7)_4$) in *m*-xylene). The reaction mixture was heated to 180 °C under a nitrogen flow in an oil bath. After 30 min the temperature was increased to 250 °C in 1 h. After 2 h at 250 °C, the pressure was slowly reduced ($P < 21$ mbar) to remove all NMP. Then, the pressure was further reduced ($P < 1$ mbar) to allow melt polycondenzation for 1 h. The polymer was cooled down to room temperature while maintaining the vacuum. To isolate the tough copolymer, the reaction mass was first cooled with liquid nitrogen. Before analysis, the polymer was dried in a vacuum oven at 50 °C for 24 h.

Injection-Molding

Samples for DMA, DSC, and compression set were prepared on an Arburg-H manual injection-molding machine. The barrel temperature was set approximately 80 °C above the melting temperature of the copolymer and the mold temperature was set on 70 °C.

Fourier Transform Infrared

FTIR spectra were recorded on a Nicolet 20SXB FTR spectrometer with a resolution of 4 cm^{-1}. The polymer was dissolved in TFA (0.1 wt %) and by spin coating, a thin polymer film ($\sim$15 μm) was formed on a silicon wafer. The polymer film was placed between two pressed KBr tablets. The FTIR data were collected between 700 and 4000 cm^{-1}. For temperature-dependent FTIR, a heating rate of 10 °C/min was used under a constant helium flow.

Synchrotron Small Angle X-ray Scattering

SAXS measurements were performed at the Dutch-Belgium (DUBBLE-BM26) beamline, at the European Synchrotron Radiation Facility (ESRF) in Grenoble. The wavelength of the beam was 1.2 Å. A two-dimensional SAXS detector was used and a q-range of 0–1.8 nm^{-1} was measured. Temperature dependent profiles were

recorded at a heating and cooling rate of 10 °C/min using a remote controlled LINKAM DSC. Two dimensionally SAXS intensity was azimuthally integrated to obtain the scattering pattern as a function of $q = 4\pi \sin \theta/\lambda$, where q is the scattering vector, 2θ the scattering angle and λ is the X-ray wavelength.

Differential Scanning Calorimetry

DSC spectra were recorded on a Perkin–Elmer DSC7 apparatus, equipped with a PE7700 computer and TAS-7 software. Dry polymer samples (5–10 mg) were heated from −50 to 250 °C at a rate of 20 °C/min. Subsequently, a cooling scan from 250 to −50 °C at a rate of 20 °C/min followed by a second heating scan under the same conditions as the first heating were performed. The melting temperature (T_m) was determined from the maximum of the endothermic peak in the second heating scan and the crystallization temperature (T_c) from the peak maximum of the exothermic peak in the cooling scan. The under-cooling of the copolymer was defined as the difference between the melting and crystallization temperature.

Viscometry

The inherent viscosity (η_{inh}) of the polymers was determined at 25 °C using a capillary Ubbelohde type 1B. The polymer solution had a concentration of 0.1 dL/g in a 1/1 (molar ratio) mixture of phenol/1,1,2,2-tetrachloroethane.

Dynamic Mechanical Analysis

The torsion behavior (storage modulus G' and loss modulus G'' as a function of temperature) was measured using a Myrenne ATM3 torsion pendulum at a frequency of 1 Hz and 0.1% strain. Before use, samples (70 × 9 × 2 mm) were dried in a vacuum oven at 50 °C overnight. Samples were cooled to −100 °C and then heated at a rate of 1 °C/min. The T_g was defined as the maximum of the loss modulus and the flow temperature (T_{flow}) as the temperature where the storage modulus reached 1 MPa. The temperature where the rubber plateau starts is denoted as the flex temperature (T_{flex}) and the storage modulus at 20 °C is given as $G'_{20\ °C}$.

Compression Set

Samples for compression set experiments were cut from injection-molded bars with a thickness of ~2.2 mm. The compression set was measured according to the ASTM 395B at 20 °C. Samples were compressed (25%) for 24 h and after 30 min of relaxation the thickness of the samples was measured. The CS was defined according to eq 1:

$$\mathrm{CS} = \frac{d_0 - d_2}{d_0 - d_1} \times 100\% \quad (1)$$

where, d_0 is thickness before compression [mm], d_1 the thickness during compression [mm] and d_2 the thickness 30 min after release of the compression [mm].

RESULTS AND DISCUSSION

Polymerization of PEO$_x$-T6T6T Block Copolymers

Segmented block copolymers based on PEO and T6T6T-dimethyl [Fig. 1(b)] were prepared via a polycondensation reaction and a titanium-based catalyst was used. As T6T6T-dimethyl units [Fig. 1(a)] have a high melting temperature (303 °C),[34] NMP was used in the first reaction step. The maximum reaction temperature was limited as PEO degrades at high temperatures. In nitrogen surroundings PEO starts to decompose at around 350 °C[35,36] and when air (oxygen) is present the decomposition starts at 220 °C.[36] Irganox 1330 was added to the reactor as antioxidant. In the first reaction step the T6T6T units were coupled to the PEO, thereby lowering the melting temperature of the T6T6T. Therefore, the polycondensation reaction could subsequently be carried out in the melt at 250 °C. During the polycondensation reaction, methanol was formed and removed. Throughout the polymerization the reaction mixture was transparent, which indicated that melt phasing did not take place. Even in the solid state the polymers were transparent, while being semicrystalline. This suggests that the T6T6T crystals were too small to scatter light. The materials had a slight yellow/brown color. Previously, it was observed that NMP in presence of a titanium catalyst at high temperature is a color source.[33] The monodispersity of the T6T6T units in polyether-T6T6T copolymer was maintained during melt synthesis and processing.[31] The polymers were difficult to dissolve and only a few solvent systems like phenol/1,1,2,2-tetrachloroethane could dissolve the copolymers. The solvent resistance of these copolymers must

Table 1. Peak Assignments of IR Bands of PEO_{2000}-T6T6T in the Wave Number Region 1580–1760 cm^{-1}

Peak (cm^{-1})	Description
1720–1730	Stretching C=O of ester bond
1660–1670	Stretching C=O of amide bond; amorphous
1630	Stretching C=O of amide bond; crystalline

have been high. The concerning copolymers had high inherent viscosities (1.4–2.5 dL/g), suggesting high molecular weight copolymers.

Fourier Transform Infrared

One elegant way of studying the crystallinity of the PEO_x-T6T6T copolymers is by FTIR spectroscopy. For these copolymers this can be done by looking at the absorption peaks of the carbonyl groups present. The absorbance band of the crystalline amide carbonyl groups is located at 1630 cm^{-1}, the amorphous amide carbonyl at 1660–1670 cm^{-1}, and the ester carbonyl at 1720–1730 cm^{-1} (Table 1).

The studied amide carbonyl absorbance bands are sensitive to the hydrogen-bonding distance between the segments. In the amorphous state this distance is larger and has a broader distance distribution compared with the crystalline state. Therefore, the amorphous amide carbonyl group is located at a high wave number and the absorbance peak is broader.

The T6T6T crystallinity can be obtained by comparing the intensity of crystalline amide carbonyl with amorphous amide carbonyl. In the melt, the amide segments are in the amorphous state and the amount of the amide carbonyl in the crystalline state is expected to be zero. Similar calculations were performed on nylon-6,6.[37] An increase in the crystallinity of nylon-6,6, expressed as an increase in the density, was linearly related to the decrease of the amorphous band and the increase of the crystalline band. In Figure 2 the FTIR spectra of PEO_{2000}-T6T6T at different temperatures are given.

The absorbance peak of the crystalline amide C=O decreased and the absorbance peak of amorphous amide C=O increased with increasing temperature. This change was particularly strong when the temperature approaches the melting temperature of the copolymer (T_m PEO_{2000}-T6T6T was 167 °C). In the melt, the peak at 1630 cm^{-1} had almost completely disappeared, while the peak at 1670 cm^{-1} was maximal. At temperatures higher than the melting temperature of the copolymer, the intensity of the 1630 cm^{-1} peak was very low and no further changes in the FTIR spectra were observed. The wave number of the amorphous amide carbonyl band increased with temperature from 1660 to 1670 cm^{-1}. The absorbance peak of the ester carbonyl shifted from 1720 to 1730 cm^{-1} with increasing temperature but the intensity was hardly affected.

The crystallinity of the rigid segments was calculated using the 1630 and 1670 cm^{-1} peak intensities (eqs 2 and 3).[33]

$$X_c = \frac{h_{\left(1630_{cm^{-1}}\right)}}{\left(C \times h_{\left(1670_{cm^{-1}}\right)}\right) + h_{\left(1630_{cm^{-1}}\right)}} \times 100\% \quad (2)$$

$$C = \frac{h_{\left(1630cm^{-1}\text{ at }50^{\circ}C\right)} - h_{\left(1630cm^{-1}\text{ melt}\right)}}{h_{\left(1670cm^{-1}\text{ melt}\right)} - h_{\left(1670cm^{-1}\text{ at }50^{\circ}C\right)}} \times 100\% \quad (3)$$

where X_c is the T6T6T crystallinity in copolymer, and $h_{(1630\ cm^{-1})}$ and $h_{(1670\ cm^{-1})}$ the height of the absorbance peak at 1630 and 1660–1670 cm^{-1} respectively.

For calculating the constant C, the peak intensities determined at 50 °C and in the melt were used. The peak intensities were taken at 50 °C as this is above the melting temperature of the crystalline PEO segments. The constant C for PEO_{2000}-T6T6T, calculated by using eq 3, had a value of 2.35. This is in agreement with

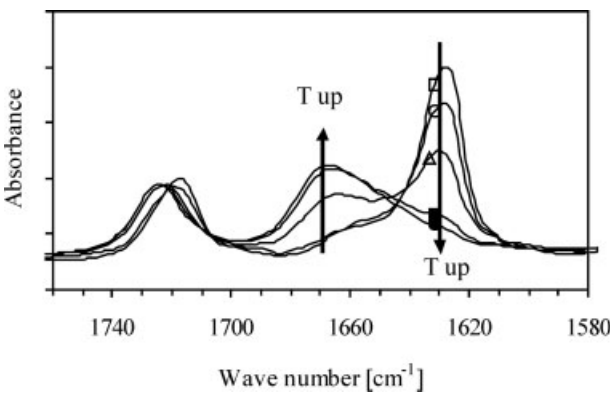

Figure 2. FTIR spectra of PEO_{2000}-T6T6T recorded at different temperatures: □, 50; ○, 100; △, 150; ■, 170; ●, 190 °C.

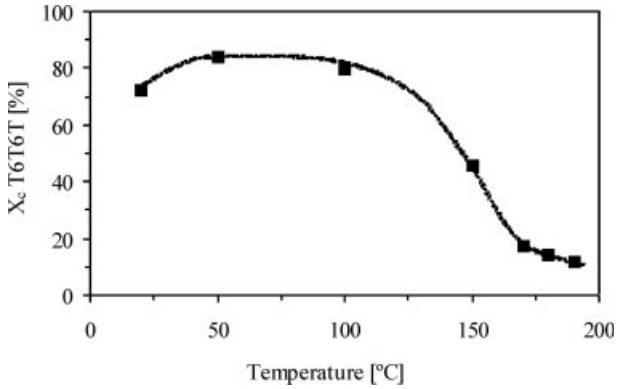

Figure 3. T6T6T crystallinity as a function of temperature for PEO_{2000}-T6T6T as measured by FTIR.

the constant found for PTMO-T6T6T copolymers.[33] The value of C was assumed to be similar for all PEO_x-T6T6T copolymers. By using eq 2 the crystallinity of the copolymers as a function of temperature was determined. In Figure 3 the T6T6T crystallinity in PEO_{2000}-T6T6T is given as a function of temperature.

From room temperature to 50 °C a small increase in T6T6T crystallinity was observed, followed by a decrease above 100 °C. The decrease was sharp at 150 °C and the crystallinity approached zero at 190 °C. For the copolymers with PEO_x is 2000 and 4600 the crystallinity at 50 °C was 84% and 87%, respectively. These high values for T6T6T crystallinities were in accordance with the values found for PTMO-T6T6T[28] and PPO-T6T6T[32] block copolymers.

The crystallinity of the T6T6T segments in PEO_{2000}-T6T6T seemed to be lower at room temperature than at 50 °C. One wonders whether the PEO crystallization affected the T6T6T crystallinity at room temperature. FTIR spectra of PEO_x-T6T6T copolymers, with different PEO segment lengths, recorded at room temperature are given in Figure 4. The PEO_{600}-T6T6T was not measured a no melt film could be made.

With increasing PEO length, the peak at 1630 cm^{-1} decreased, the peak at 1660 cm^{-1} increased and the peak at 1720 cm^{-1} remained constant. This suggests that at room temperature the crystallinity of the T6T6T segments decreased as the PEO length increased. To study the influence of PEO crystallinity on the T6T6T crystallinity near room temperature in more detail, FTIR spectra of PEO_{4600}-T6T6T were recorded in a temperatures range of 20–70 °C (Fig. 5).

On heating from 20 to 50 °C, the solution cast films showed a decrease in the peak intensity of

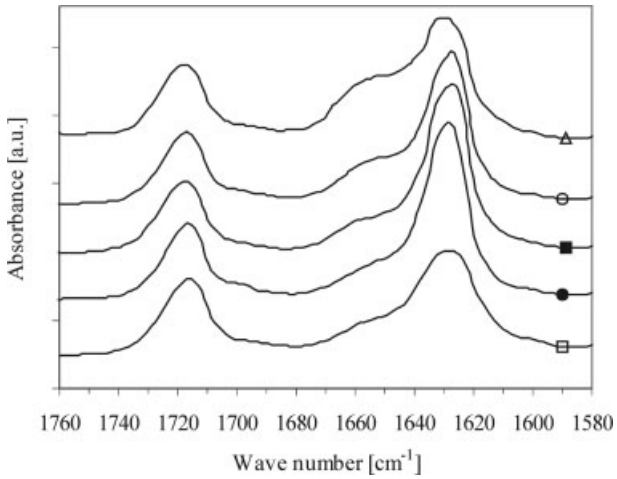

Figure 4. FTIR spectra of PEO_x-T6T6T recorded at room temperature with different PEO_x lengths (x): ●, 1500; ■, 2000; ○, 3400; △, 4600.

1660 cm^{-1}. Above 50 °C the peak intensity did not change anymore. In Figure 6 the T6T6T crystallinity of PEO_{4600}-T6T6T is given as a function of the temperature.

On heating from 20 to 50 °C the T6T6T crystallinity increased and at temperatures above 50 °C the crystallinity decreased slowly. The maximum T6T6T crystallinity at 50 °C coincided with the melting temperature of PEO_{4600} crystals in the copolymer (T_m PEO = 53 °C). In the subsequent cooling scan from 70 to 20 °C the T6T6T crystallinity only increased. These results suggest that the T6T6T crystallization in a solution-cast film was not complete. At higher temperature, when PEO crystals were molten, the amorphous phase was more mobile and more T6T6T segments were able to crystallize.

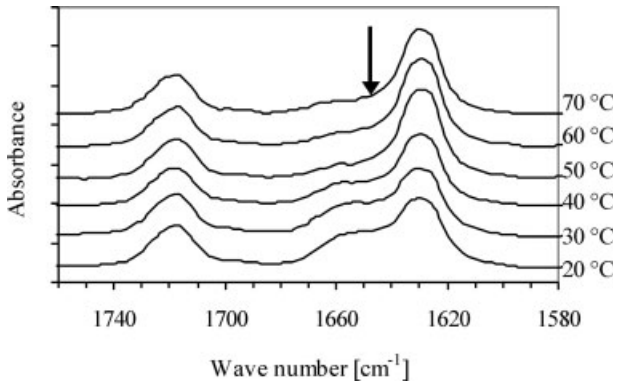

Figure 5. FTIR spectra of PEO_{4600}-T6T6T recorded at different temperatures (20–70 °C) for the wave number region 1580–1760 cm^{-1}.

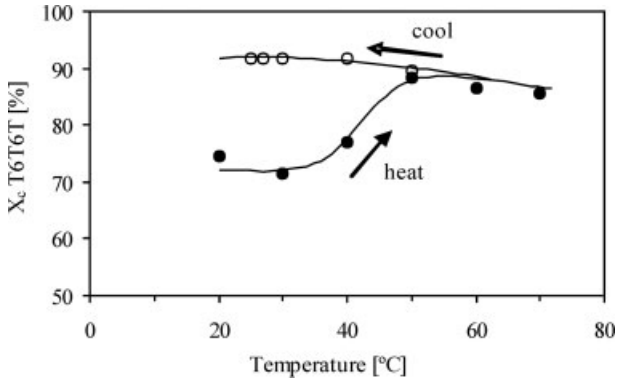

Figure 6. T6T6T crystallinity of PEO_{4600}-T6T6T as a function of temperature at 10 °C/min as measured by FTIR: ●, heating and ○, cooling cycle.

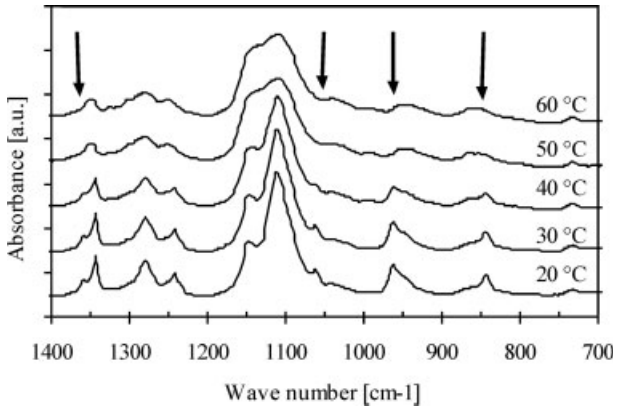

Figure 7. FTIR spectra of PEO_{4600}-T6T6T recorded at different temperatures for the wave number region 700–1400 cm^{-1}.

With FTIR it was also possible to study the melting and crystallization of the PEO segments. The absorbance peaks of PEO_{4600}-T6T6T in the wave number region between 700 and 1400 cm^{-1} were taken at different temperatures (Fig. 7). With increasing temperature some absorbance peaks shifted and these peaks are indicated by arrows. The assignments and descriptions of the changing absorbance peaks are given in Table 2. From these spectra it is clear that the PEO crystals in the PEO_{4600}-T6T6T copolymer melted at about 50 °C. The changes of the absorbance peaks on melting were too small to calculate the PEO crystallinity.

Assignments and description of the most distinguishable FTIR absorbance peaks of amorphous and crystalline PEO.[38]

Synchrotron Small Angle X-ray Scattering

SAXS experiments were performed to obtain information about the morphology of the crystallites in segmented block copolymers. The long-spacing (L) can be determined from SAXS measurements on materials that possess a lamellar structure. This spacing corresponds to the lamellar thickness plus the thickness of the interlamellar (amorphous) region. The L-spacing is an average value of a two dimensional ordering of the lamellae in the matrix.

Temperature modulated SAXS studies were carried out on PEO_{1000}-T6T6T. According to AFM the T6T6T crystallites in polyether-T6T6T copolymers have a ribbon-like structure with the ribbons randomly oriented.[28] When a ribbon-like structure is present and the ribbons randomly oriented with respect to other ribbons than the L-spacing in both the thickness and the width direction might have a similar value.

In the intensity plots, where the scattering intensity $I(q)$ was given as a function of the scattering vector q, a scattering maximum was observed which indicated the presence of phase-separated domains (Fig. 8). The small drop in intensity in the beginning of the curve was due to scattering of the beam. The L-spacing can be derived from the scattering data;

$$L = \frac{2\pi}{q} \tag{4}$$

As the temperature increased, the scattering maximum and intensity decreased at the same time. These changes were due to melting of the T6T6T crystals. Above the melting temperature

Table 2. Assignments and Description of the Most Distinguishable FTIR Absorbance Peaks of Amorphous and Crystalline PEO[38]

Amorphous PEO (cm^{-1})	Crystalline PEO (cm^{-1})	Description
1350	1360/1343	Wagging CH_2
1250/1280	1240/1280	Twisting CH_2
	1150	Stretching C—O, Stretching C—C
1110	1111	Stretching C—O
	1061	Stretching C—O, Stretching C—C, rocking CH_2
	960	Rocking CH_2
950	950	Stretching C—O, rocking CH_2
860	843	Rocking CH_2

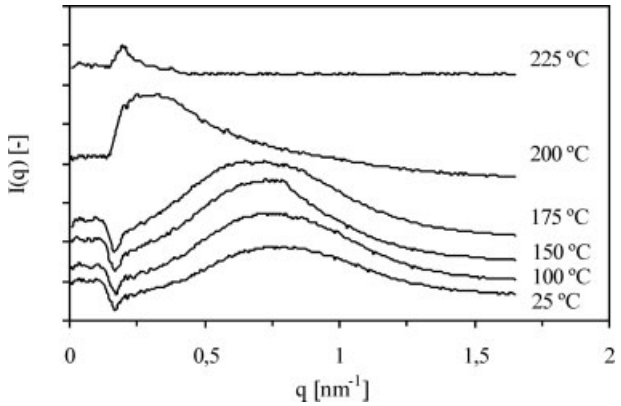

Figure 8. SAXS curves of PEO_{1000}-T6T6T at different temperatures.

of the copolymer (T_m of PEO_{1000}-T6T6T is 195 °C) there was no peak observed anymore, which indicates that there was no crystalline order present in the melt.

The SAXS curves showed only one broad scattering maximum. Therefore, it seemed that there was only one L-spacing for both the thickness and width direction. This suggests that the T6T6T ribbons had a comparable crystalline thickness and width values. In Figure 9 the long-spacing of PEO_{1000}-T6T6T as a function of temperature was given, during a heating and cooling cycle.

The long-spacing of PEO_{1000}-T6T6 at 25 °C was 8.2 nm and remained almost constant upon heating till a temperature of ~170 °C. This was due to the monodisperse segments that all melt at the same temperature. As the temperature reached the melting temperature of the copolymer the L-spacing increased tremendously. Upon cooling, the L-spacing decreased again with a temperature lag of 30 °C. This small temperature lag indicates a high rate of crystallization of the monodisperse segments. At 25 °C the L-spacing was 9.9 nm with was close to the starting value. When a ribbon-like crystalline structure is present, it is assumed that the thickness and width L-spacing values are comparable. So, it was not possible to calculate a crystallite thickness from these 2D-SAXS data.

Differential Scanning Calorimetry

The PEO_x-T6T6T copolymers had a melt transition of T6T6T and possibly a melt transition of the PEO segments. By using DSC the melting and crystallization temperatures and enthalpies of PEO_x-T6T6T copolymers were determined. The second heating scan and first cooling scan of the copolymers are plotted in Figure 10 and the corresponding results are given in Table 3.

The copolymer with a PEO length of 600 g/mol showed no melting peak of PEO. Apparently these segments were too short to crystallize. As the PEO length increased the melting peak and enthalpy of the PEO crystals increased, which indicates that the PEO crystallinity increased.

For the copolymers with PEO_{3400} and PEO_{4600} no crystallization peak of T6T6T is observed as most likely the T6T6T concentration (>15 wt %) is too low to give a measurable peak. The T6T6T crystallization peak for the PEO_{2000} copolymer was already very weak and the T_c value not accurate and as a result of this the $T_m - T_c$ for this copolymer also not accurate. The melting enthalpy of T6T6T in the copolymer was lower than observed for the T6T6T-dimethyl segments (152–180 J/g). Furthermore, the melting enthalpy of T6T6T showed a decrease as the PEO concentration increased. The T6T6T melting enthalpy of the PEO_{1000} copolymer seems to be on the high side. The decrease in melting enthalpy suggests that the T6T6T segments were not fully crystallized and/or that due to exothermic mixing energies the melting endotherms were not simply related to crystallinities. The copolymers had low under-cooling values and this suggest that the monodisperse crystallizable rigid segments crystallized very fast.

Dynamic Mechanical Analysis

The storage and loss moduli of the PEO_x-T6T6T copolymers, determined by DMA measurements, are plotted as a function of temperature in Fig-

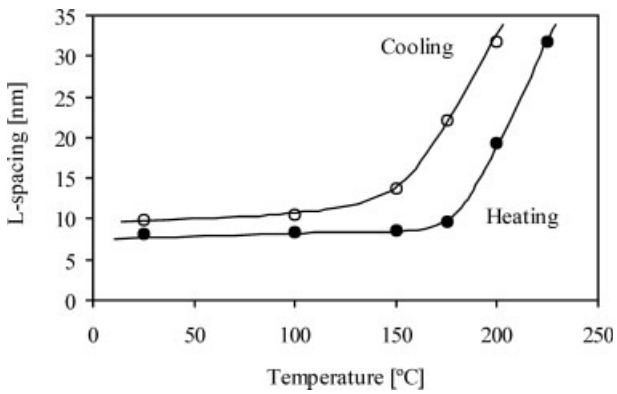

Figure 9. Long-spacing of PEO_{1000}-T6T6T as a function of temperature, at 10 °C/min: ●, heating; ○, cooling cycle.

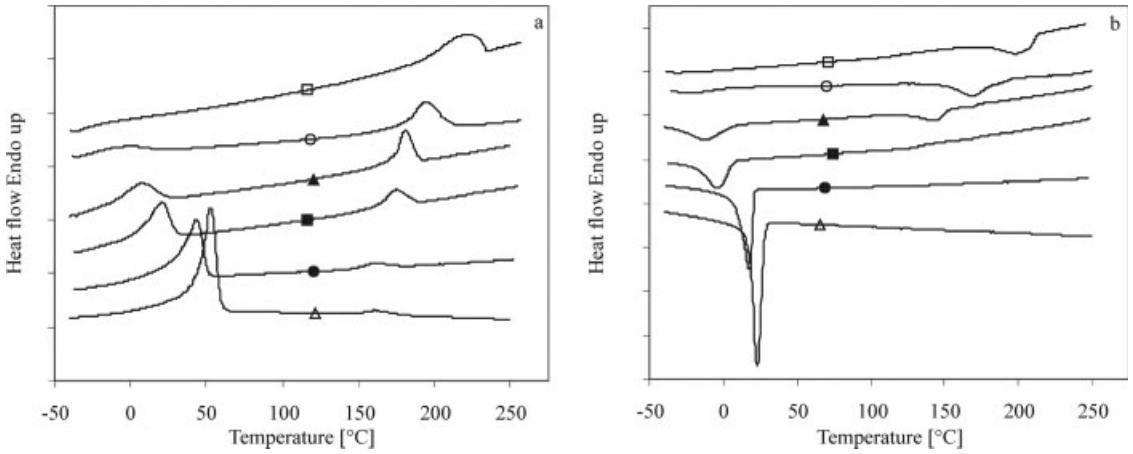

Figure 10. DSC second heating scan (a) and first cooling scan (b) of PEO_x-T6T6T with different PEO lengths (x): □, 600; ○, 1000; ▲, 1500; ■, 2000; ●, 3400; △, 4600.

ure 11 and the corresponding data are given in Table 4. Of PEO_{1500}-T6T6T and PEO_{4600}-T6T6T were for clarity the lines in Figure 11 left out.

All copolymers had a wide and almost temperature independent rubbery plateau and a sharp melting temperature. This large service temperature is typical for copolymers with crystallizable segments of monodisperse length. The storage modulus and flow temperature increased with decreasing PEO_x length due to an increased T6T6T content.

The synthesized PEO_x-T6T6T copolymers had a high inherent viscosity (>1.4 dL/g) and, therefore, a relatively high molecular weight is expected (Table 4).

Low Temperature Properties

The plot of the loss moduli as a function of the temperature of the PEO_x-T6T6T copolymers [Fig. 11(b)] show a low T_g, which originates from the polyether phase. A T_g of an amorphous T6T6T phase was not observed (T_g of nylon-6, T is 125 °C[39]), which suggests that there was no separate amorphous T6T6T phase present in the copolymers. Both the T_g and flex temperature (T_{flex}) of PEO_x-T6T6T copolymers changed with the PEO segment length (Fig. 12).

With increasing PEO segment length the T_g decreased. The relation between the T_{flex} and the PEO segment length was more complex. The T_g of crosslinked segments decreased with increasing crosslink density.[40] A complicating factor was that the longer PEO segments were semi crystalline at low temperatures and this PEO crystalline phase must have had an effect on crosslink density and thus on the T_g. The PEO segments in copolymers had higher T_g than the T_g of the PEO prepolymers (−72 – −65 °C[38]). This effect was due to the reduced mobility of a bound segment. When the T_g of the prepolymers was corrected for the reduced mobility, the value was close to the T_g of the PEO in the copolymers. The high T_g for PEO_{600} can be explained by the high physical crosslink density in this copolymer. The T_g of the polyether

Table 3. DSC Results of PEO_x-T6T6T Copolymers

			PEO		T6T6T			
PEO Length (x) (g/mol)	Conc. T6T6T (wt %)	Conc. PEO (wt %)	T_m (°C)	ΔH_m (J/g PEO)	T_m (°C)	ΔH_m (J/g T6T6T)	T_c (°C)	$T_m - T_c$ (°C)
600	51.0	49.0	–	–	219	81	201	18
1000	38.4	61.6	−2	20	195	104	169	26
1500	29.4	70.6	7	49	181	81	144	37
2000	23.8	76.2	21	53	167	73	161	6
3400	15.5	84.5	44	89	162	37	–	–
4600	11.9	88.1	53	103	161	42	–	–

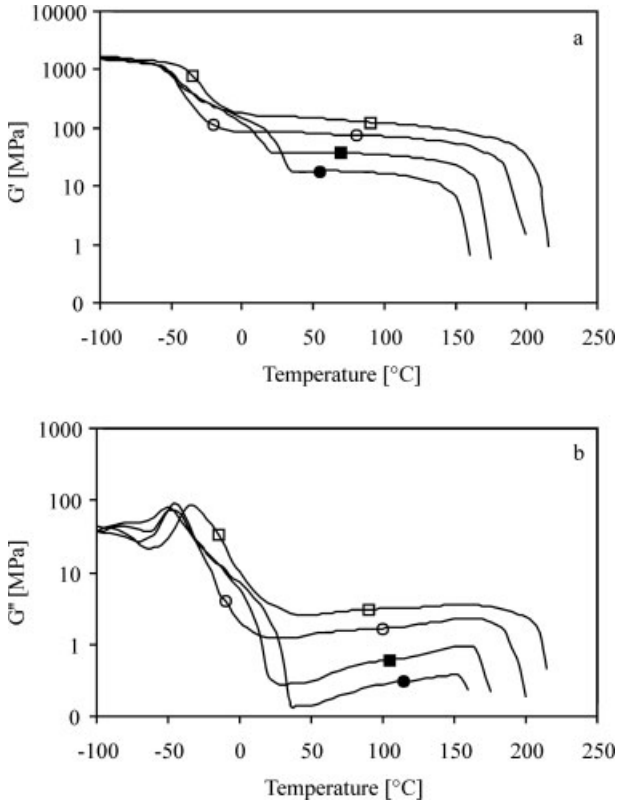

Figure 11. Storage (a) and loss (b) modulus of PEO_x-T6T6T with different PEO lengths (x): □, 600; ○, 1000; ■, 2000; ●, 3400.

phase increased also with increasing amount of amorphous rigid segments dissolved in the polyether phase. Since the observed T_g's of PEO_x-T6T6T copolymers were low, it suggests that only a small amount of amorphous T6T6T was dissolved in the PEO phase. This is in accordance with the FTIR results, indicating that the T6T6T crystallization was almost complete.

The shoulder in the storage modulus after the T_g was a result of the melting of the PEO crystalline phase [Fig. 11(a)]. An increase in PEO length leads to a higher PEO melting temperature and crystallinity (Table 3). The height of the shoulder at about 0 °C increased for the longer PEO segments despite the lower T6T6T content. The PEO crystallites increased the modulus at that temperature. The T_{flex}, defined as the temperature where the rubbery plateau starts, was related to the T_g or melting temperature of PEO (Fig. 12). In the case of a complete amorphous PEO phase, the T_{flex} would have followed the same trend as the T_g, indicated by the dotted line in Figure 12. When the PEO is partly crystalline the T_{flex} corresponds to the T_m of the PEO.

Storage Modulus

The modulus of the rubbery plateau at 55 °C of PEO_x-T6T6T copolymers decreased with decreasing T6T6T content (Fig. 13, Table 4). As the copolymers had a comparable T6T6T crystallinity one can conclude that the modulus increased with crystalline content. With an increase in T6T6T content, the physical crosslink density and the reinforcing filler effect of the crystalline domains increased. The moduli of the rubbery plateau of PEO-T6T6T copolymers were similar to the corresponding moduli of PPO-T6T6T[32] and PTMO-T6T6T[28] copolymers. This suggests that the reinforcing filler effect of the T6T6T crystallites was comparable in all three types of polyether-T6T6T copolymers. The strong increase in modulus of the polyether-T6T6T copolymers could be well described by the fiber composite model of Halpin–Tsai.[32,33] This model suggests that the crystalline ribbons in the copolymer can be considered as reinforcing nanofillers for the amorphous matrix.

Besides the T6T6T concentration, the storage modulus was also influenced by the presence of a semicrystalline PEO phase. The storage modulus of PEO_x-T6T6T copolymers at 20 °C increased at low T6T6T contents when the PEO

Table 4. Dynamic Mechanical and Elastic Properties of PEO_x-T6T6T Copolymers

PEO Length (x) (g/mol)	Conc. T6T6T (wt %)	Conc. PEO (wt %)	η_{inh} (dL/g)	T_g (°C)	T_{flex} (°C)	$G'_{20\ °C}$ (MPa)	$G'_{55°C}$ (MPa)	T_{flow} (°C)	$CS_{25\%}$ (20°C) (%)	$CS_{25\%}$ (70°C) (%)
600	51.0	49.0	1.4	−33	−4	160	147	216	34	55
1000	38.4	61.6	1.4	−45	−13	86	80	199	22	–
1500	29.4	70.6	1.5	−46	7	57	58	180	23	–
2000	23.8	76.2	2.1	−48	20	38	38	174	17	45
3400	15.5	84.5	2.5	−50	33	72	18	159	49	–
4600	11.9	88.1	2.1	−45	55	201	12	154	32	–

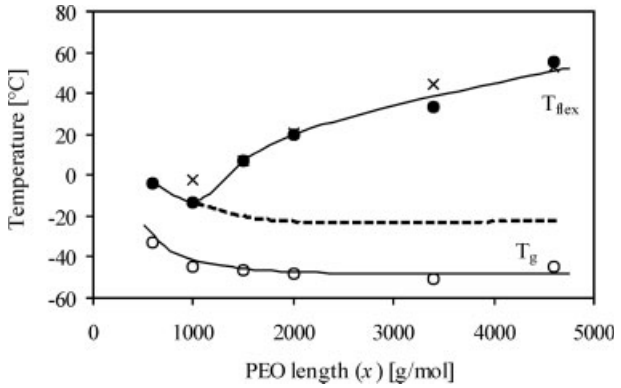

Figure 12. Transitions of the soft phase in PEO_x-T6T6T as a function of PEO length (x): ○, glass transition temperature; ●, flex temperature; ×, melting temperature of PEO (DSC results) (dotted line: expected flex temperature in absence of PEO crystallization).

segment length is >2000 g/mol. With these PEO segments the PEO melting temperature was above 20 °C, which resulted in a higher $G'_{20\ °C}$. Because of the increasing PEO melting temperature with increasing PEO length, it was not possible to create a PEO_x-T6T6T copolymer having a low modulus at room temperature ($G' < 15$ MPa). The modulus of the copolymers had in the plateau region a small decrease in modulus (about 0.3%/°C) and such a small decrease is typical for monodisperse hard segments.[27,28,30,32,33]

Flow Temperature

The flow temperature of PEO_x-T6T6T copolymers decreased with increasing PEO segment content. The melting temperature of the copolymers, measured with DSC, corresponded well to the flow temperature determined with DMA. The decrease in melting temperature with increasing PEO length can be explained by the solvent effect theory proposed by Flory, which states that the amorphous phase acts as a solvent for the crystallizable phase.[41,42] An increase in amorphous phase content leads to a decrease in the melting temperature of the copolymer. According to the Flory solvent theory, the melting temperature depression by the presence of a solvent depends on the melting enthalpy of the crystalline segment, the ratio of molar volumes of the solvent and the crystalline segment and the interaction parameter between the segments.

In Figure 14, the melting temperatures of the polyether-T6T6T copolymers are plotted against the volume fraction of polyether (v_s). The densities of PEO, PPO, and PTMO, respectively, 1.13, 1.00, and 0.98 g/cm^3, and the calculated density of T6T6T (1.32 g/cm^3) were used to determine the volume fraction of polyether in the copolymers.[43] At a similar PEO concentration, the flow temperature of PEO-T6T6T was lower that of PTMO-T6T6T[28] or PPO-T6T6T[32] copolymers. This suggests that PEO was more effective in lowering the melting temperature than PPO and PTMO. The relationship developed by Flory can only be applied for polymer systems containing low amounts of solvent and, therefore, could not be used for our high PEO-containing systems.

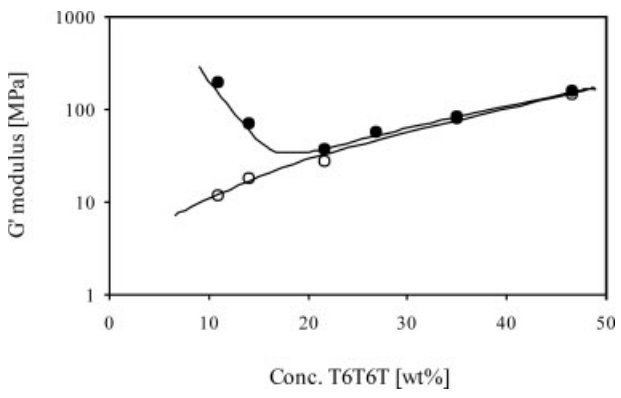

Figure 13. Storage modulus as a function of the T6T6T content: ●, 20 °C; ○, 55 °C.

Compression Set

A measure of elasticity of polymers is the compression set. The compression set (CS) test

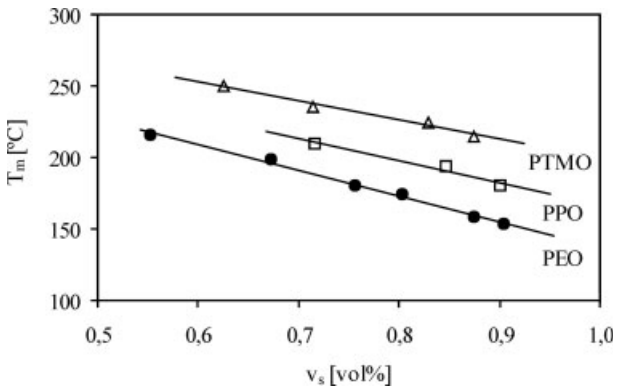

Figure 14. Melting temperature of polyether-T6T6T copolymers as a function of volume fraction of polyether: ●, PEO; □, PPO[33]; △, PTMO.[27]

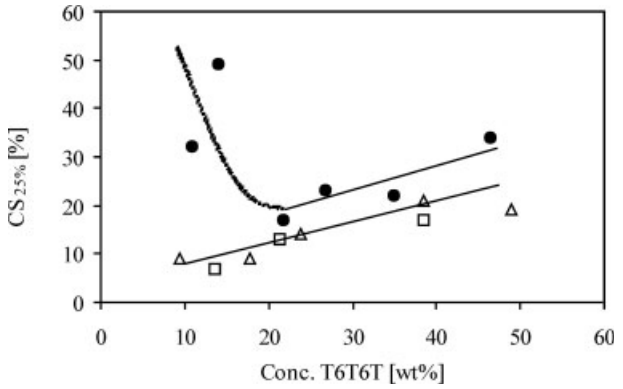

Figure 15. Compression set at 20 °C of polyether-T6T6T copolymers as a function of the T6T6T content: ●, PEO; □, PPO[33]; △, PTMO.[27]

determines the recovery of a material after compression. In segmented block copolymers two relaxation processes are involved; an elastic and visco-elastic process and a process of plastic deformation.[44,45] It was found that at room temperature the CS values of segmented block copolymers with crystallizable segments slightly decreased in time, indicating that the effect of visco-elastic deformation in this CS test was small. Moreover, the stress relaxation experiments showed that the copolymers relaxed at a low rate. At higher temperatures, the visco-elastic relaxation was faster.[45] So, for these copolymers the CS at room temperature is mainly determined by the plastic deformation.

Generally, the CS values of segmented block copolymers with monodisperse rigid segments increase with increasing rigid segment concentration on the condition that the polyether phase is completely amorphous.[28,32,33] In Figure 15 the CS values of polyether-T6T6T copolymers is given as a function of the T6T6T concentration.

At low T6T6T contents, the CS values of PTMO- and PPO-T6T6T copolymers were very low. However, the CS values of PEO_x-T6T6T copolymers at room temperature increased when the T6T6T content was below 20 wt %. In this case, the PEO segment length was >2000 g/mol and these long PEO segments were partly crystalline and had a melting temperature above 20 °C (Table 3). The crystalline PEO phase restricted the recovery and thus the elasticity of the copolymer at room temperature. When the CS was measured at 70 °C, above the PEO melting temperature, the high CS values at low T6T6T contents were absent (Table 4). The PPO segments do not crystallize and the PTMO segments can crystallize but the melting temperature of these crystals is below room temperature. Thus, the CS values of PPO-T6T6T and PTMO-T6T6T copolymers were at room temperature not influence by the presence of polyether crystals.

The PEO crystalline phase interfered not only in the CS at 20 °C but also in the modulus at 20 °C. The relationship between the modulus and compression is characteristic for segmented block copolymers. However, the PEO_x-T6T6T copolymers had a rather complex modulus-CS relationship (Fig. 16). The CS values of copolymers with a PEO length of 600–2000 g/mol decreased with decreasing storage modulus. This behavior is familiar for other polyether-T6T6T copolymers.[28,32,33] However, the copolymers with PEO_{3400} and PEO_{4600} had an increased modulus and increased CS values. No further decrease in CS values with decreasing modulus, which was due to the presence of high melting PEO crystals. This indicates that at room temperature the copolymers with PEO_{3400} and PEO_{4600} had poor elastic properties.

CONCLUSIONS

Segmented block copolymers based on PEO flexible segments and monodisperse crystallizable tetra-amide segments (T6T6T) had been synthesized via a high temperature polycondensation reaction. A copolymer series was prepared where the molecular weight of PEO_x segments was varied from 600 to 4600 g/mol, thereby changing the T6T6T concentration from 51.0 to

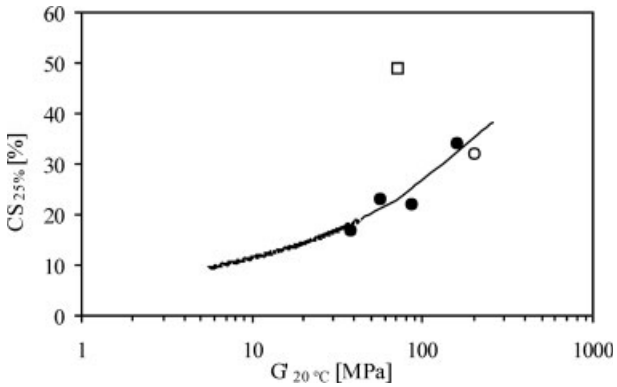

Figure 16. Compression set at 20 °C of PEO_x-T6T6T copolymers as a function of the storage modulus at 20 °C: ●, $PEO_{600\text{-}2000}$; □, PEO_{3400}; ○, PEO_{4600}; —, expected trend in absence of PEO crystallinity.

11.9 wt %. The copolymers had a high molecular weight, were melt-processable, solvent resistant and transparent. By using monodisperse rigid segments the crystallization of the copolymers was according to FTIR measurements fast and almost complete, the T6T6T crystallinity was high (>84%). Besides, the T6T6T crystallinity remains high up to ~30 °C below the melting temperature of the copolymer. SAXS experiments reveal for PEO_{1000}-T6T6T a long-spacing of 8.2 nm, which remained almost constant upon heating due to the use of monodisperse segments.

DMA experiments showed that the materials had a low T_g, a broad and almost temperature independent rubbery plateau, and a sharp melting temperature. Because of the use of monodisperse rigid segments the phase-separation between the hard and soft phase was almost complete and only a small amount of noncrystallized rigid segments was expected to be dissolved in the PEO matrix. As the T6T6T content increased (11.9–51.0 wt %), the storage modulus of the rubbery plateau (12–159 MPa) and the flow temperature (154–216 °C) increased.

The PEO melting temperature and enthalpy increased when the molecular weight of the PEO segments increased. When the PEO length is >2000 g/mol the melting temperature of the PEO crystals was above room temperature, a reduced elasticity of the copolymer was the result. So, due to the PEO crystallization in the PEO_x-T6T6T copolymers it was impossible to create a low modulus material ($G' < 15$ MPa).

The PEO-T6T6T copolymers had similar modulus-composition behavior as PPO-T6T6T and PTMO-T6T6T copolymers, indicating that the reinforcing effect of the T6T6T crystals was comparable. However, at equal T6T6T concentrations the melting temperature of the polyether-T6T6T copolymers decreased in the order of PTMO < PPO < PEO.

The present research was financed by the Dutch Polymer Institute (DPI, The Netherlands), project #313. The authors thank the ESRF (European Synchrotron Radiation Facility) at Grenoble (Fr.) for the use of their facilities and Brass and Heunen for their assistance.

REFERENCES AND NOTES

1. Gebben, B. J Membr Sci 1996, 113, 323.
2. Metz, S. J.; Mulder, M. H. V.; Wessling, M. Macromolecules 2004, 37, 4590.
3. Stroeks, A.; Dijkstra, K. Polymer 2001, 42, 117.
4. Bondar, V. I.; Freeman, B. D.; Pinnau, I. J Polym Sci Part B: Polym Phys 1999, 37, 2463.
5. Bondar, V. I.; Freeman, B. D.; Pinnau, I. J Polym Sci Part B: Polym Phys 2000, 38, 2051.
6. Lee, D.; Lee, S.; Kim, S.; Char, K.; Park, J. H.; Bae, Y. H. J Polym Sci Part B: Polym Phys 2003, 41, 2365.
7. Schneider, N. S.; Langlois, D. A.; Byrne, C. A. Polym Mater Sci Eng 1993, 69, 249.
8. Chen, C. T.; Eaton, R. F.; Chang, Y. J.; Tobolsky, A. V. J Appl Polym Sci 1972, 16, 2105.
9. Schneider, N. S.; Illinger, J. L.; Karasz, F. E. J Appl Polym Sci 1993, 47, 1419.
10. Yilgör, I.; Yilgör, E. Polymer 1999, 40, 5575.
11. Claase, M. B.; Grijpma, D. W.; Mendes, S. C.; De Bruijn, J. D.; Feijen, J. J Biomed Mater Res A 2003, 64, 291.
12. Deschamps, A. A.; Grijpma, D. W.; Feijen, J. J Controlled Release 2003, 87, 302.
13. Deschamps, A. A.; Van Apeldoorn, A. A.; De Bruijn, J. D.; Grijpma, D. W.; Feijen, J. Biomaterials 2003, 24, 2643.
14. Van Dorp, A. G. M.; Verhoeven, M. C. H.; Koerten, H. K.; Van Blitterswijk, C. A.; Ponec, M. J Biomed Mater Res 1999, 47, 292.
15. Deschamps, A. A.; Claase, M. B.; Sleijster, W. J.; De Bruijn, J. D.; Grijpma, D. W.; Feijen, J. J Controlled Release 2002, 78, 175.
16. Van Dijkhuizen-Radersma, R.; Metairie, S.; Roosma, J. R.; De Groot, K.; Bezemer, J. M. J Controlled Release 2005, 101, 175.
17. Van Dijkhuizen-Radersma, R.; Roosma, J. R.; Kaim, P.; Metairie, S.; Peters, F.; De Wijn, J.; Zijlstra, P. G.; De Groot, K.; Bezemer, J. M. J Biomed Mater Res A 2003, 67, 1294.
18. Fakirov, S.; Gogeva, T. Makromol Chem 1990, 191, 603.
19. Fakirov, S.; Gogeva, T. Makromol Chem 1990, 191, 615.
20. Fakirov, S.; Goranov, K.; Bosvelieva, E.; Du Chesne, A. Makromol Chem 1992, 193, 2391.
21. Miller, J. A.; Lin, S. B.; Hwang, K. K. S.; Wu, K. S.; Gibson, P. E.; Cooper, S. L. Macromolecules 1985, 18, 32.
22. Harrell, L. L. Macromolecules 1969, 2, 607.
23. Versteegen, R. M.; Kleppinger, R.; Sijbesma, R. P.; Meijer, E. W. Macromolecules 2006, 39, 772.
24. Versteegen, R. M.; Sijbesma, R. P.; Meijer, E. W. Macromolecules 2005, 38, 3176.
25. Van der Schuur, J. M.; Noordover, B.; Gaymans, R. J. Polymer 2006, 47, 1091.
26. Biemond, G. J. E.; Brasspenning, K.; Gaymans, R. J. J Appl Polym Sci, in press.
27. Niesten, M. C. E. J.; Feijen, J.; Gaymans, R. J. Polymer 2000, 41, 8487.
28. Krijgsman, J.; Husken, D.; Gaymans, R. J. Polymer 2003, 44, 7573.
29. Krijgsman, J.; Gaymans, R. J. Polymer 2004, 45, 437.

30. Husken, D.; Krijgsman, J.; Gaymans, R. J. Polymer 2004, 45, 4837.
31. Van der Schuur, J. M.; Feijen, J.; Gaymans, R. J. Polymer 2005, 46, 4584.
32. Van der Schuur, J. M.; Gaymans, R. J. J Polym Sci Part A: Polym Chem 2006, 44, 4769.
33. Biemond, G. J. E.; Feijen, J.; Gaymans, R. J. J Appl Polym Sci 2007, 105, 951.
34. Krijgsman, J.; Husken, D.; Gaymans, R. J. Polymer 2003, 44, 7043.
35. Cameron, G. G.; Ingram, M. D.; Qureshi, M. Y.; Costa, L.; Camino, G. Eur Polym J 1989, 25, 779.
36. Costa, L.; Gad, A. M.; Camino, G.; Cameron, G. G.; Qureshi, M. Y. Macromolecules 1992, 25, 5512.
37. Zbinden, R. Infrared Spectroscopy of High Polymers; Academic Press: New York, 1964.
38. Bailey, J. F. E.; Koleske, J. V. Poly(ethylene oxide); Academic Press: New York, 1976.
39. Morgan, P. W.; Kwolek, S. L. Macromolecules 1975, 8, 104.
40. Cowie, J. M. G. Polymers: Chemistry & Physics of Modern Materials; Chapman & Hall: Cheltenham, 1991.
41. Flory, P. J. Principles of Polymer Chemistry; Cornell University Press: Ithaca, 1967.
42. Flory, P. J. Trans Faraday Soc 1955, 51, 848.
43. Van Krevelen, D. W. Properties of Polymers; Elsevier Science: New York, 1990.
44. Van der Schuur, J. M.; De Boer, J.; Gaymans, R. J. Polymer 2005, 46, 9243.
45. Biemond, G. J. E. Ph.D. Thesis, University of Twente, Enschede, 2006.